Research Square

Preprints are preliminary reports that have not undergone peer review.
They should not be considered conclusive, used to inform clinical practice,
or referenced by the media as validated information.

The Sperm Rheotaxis Index for Assessing Sperm Function and Male Infertility Using a Microfluidic Platform

Boyang Zhang
Changhai Hospital
Hui Zhang
Changhai Hospital
Guanyu Ren
Changhai Hospital
Chenghua Yang
Changhai Hospital
Jian Xu
Changhai Hospital
Xinlong Wang
Changhai Hospital
Weihao Sun
Changhai Hospital
Shuguang Piao
Changhai Hospital
Wenjie Chen
Changhai Hospital
Xinyu Yang
Changhai Hospital
Jiaxin Liu
Changhai Hospital
Lei Wang
Changhai Hospital
Zhiyong Liu
546882215@qq.com

Changhai Hospital

Research Article

Keywords:

Posted Date: November 20th, 2026

DOI: https://doi.org/10.21203/rs.3.rs-11573993/v1

License: This work is licensed under a Creative Commons Attribution 4.0 International License.
Read Full License

Title: The Sperm Rheotaxis Index for Assessing Sperm Function and Male Infertility Using a Microfluidic Platform

Boyang Zhang [a,c,1], Hui Zhang [b,1], Guanyu Ren [a, 1], Chenghua Yang [a], Jian Xu [b], Xinlong Wang [a], Weihao Sun [a], Shuguang Piao [a], Wenjie Chen [a], Xinyu Yang [b], Jiaxin Liu [a,*], Lei Wang [a,*], Zhiyong Liu [a,b,*]

[a]Department of Urology, The First Affiliated Hospital of Naval Medical University, Shanghai, China.

[b]Sperm Bank, The First Affiliated Hospital of Naval Medical University, Shanghai, China

[c]Department of Urology, 921 Hospital of Joint Logistics Support Force People's Liberation Army of China (The Second Affiliated Hospital of Hunan Normal University), Changsha, China

* Corresponding author. Department of Urology, The First Affiliated Hospital of Naval Medical University, Shanghai, China.
E-mail: 546882215@qq.com (Zhiyong Liu)
[1] Authors contribute equal in this work.

Keywords: sperm rheotaxis, microfluidic, sperm motility, male infertility, sperm function

Abstract:

Background: Male infertility accounts for nearly half of infertility cases worldwide. Conventional semen analysis provides limited information about sperm function. Sperm rheotaxis, the ability of sperm to swim against fluid flow, is a distinctive form of sperm motility that contributes to natural fertilization.

Objective: To establish the Sperm Rheotaxis Index (SRI) using a microfluidic platform and evaluate its potential as a functional biomarker for assessing sperm function and male infertility.

Methods: A bioinspired microfluidic platform was developed to mimic the mucosal folds of the female reproductive tract and generate physiologically relevant shear stress, enabling real-time visualization and quantitative assessment of sperm rheotaxis. SRI was calculated using image analysis to quantify directional sperm motility under controlled flow

conditions. In a cohort of 86 participants, associations between SRI, conventional motility parameters, and the DNA fragmentation index were evaluated. Receiver operating characteristic analysis was used to assess the discriminatory performance of SRI relative to conventional motility parameters, including among men with normal sperm motility.

Results: SRI showed strong positive correlations with several sperm motility parameters and a negative correlation with the DNA fragmentation index. Lower SRI values were observed in individuals with male infertility-related conditions. SRI demonstrated better discriminatory performance than conventional motility parameters, with an area under the curve (AUC) of 0.77. Among men with normal sperm motility, SRI also distinguished fertile from subfertile individuals (AUC = 0.70). These findings support the potential of SRI as a functional biomarker that complements conventional semen analysis in the assessment of male fertility.

1. Introduction

Infertility affects approximately 8–12% of couples of reproductive age worldwide, about half of these cases are attributed to male-related causes, including abnormalities in sperm quality, quantity, or function[1]. Clinically, oligozoospermia, asthenozoospermia, and varicocele are among the most prevalent conditions that impair semen quality and compromise male fertility potential[2]. Notably, a considerable proportion of infertile men are display normal conventional semen parameters but possess subtle physiological dysfunctions that impair fertilization[3]. However, routine semen analysis traditionally overlooks these functional deficits and lacks the sensitivity to assess fertilization-related competence[4]. Earlier functional assays—such as the human zona pellucida binding test and the hamster oocyte penetration assay—were labor-intensive, subject to operator variability, and have largely been discontinued in clinical settings. Currently, there is a marked absence of standardized, reproducible methods for evaluating sperm function in routine diagnostics[5].

During natural reproduction, an ejaculate typically delivers up to hundreds of millions of sperm cells into the female reproductive tract. However, only a small fraction of these sperm can progress further due to several physiological barriers. These include the acidic vaginal environment, cervical mucus, the narrow cervical canal, and the complex structure of the uterotubal junction and fallopian tubes[6]. As a result, fewer than 1,000 sperm cells usually reach the isthmus of the fallopian tube. At this site, they undergo capacitation and begin actively navigating toward the oocyte (Figure 1a)[7]. To overcome these obstacles, sperm cells

rely on specialized guidance mechanisms, including chemotaxis, rheotaxis, and thermotaxis, which together facilitate directional migration and enable successful fertilization[8].

Sperm rheotaxis refers to the ability of sperm cells to orient and swim upstream. It responses to shear stress gradients within dynamic fluid environments. As a fundamental biophysical mechanism, it facilitates directed migration through the female reproductive tract and plays a pivotal role in enabling fertilization[9]. Notably, sperm rheotaxis has been associated with enhanced progressive motility, improved DNA integrity, and higher embryogenesis rates in assisted reproductive technologies (ART)[10]. However, conventional in vitro assessment tools, such as computer-assisted semen analysis (CASA), operate under static conditions. These conditions fail to replicate the fluid dynamics and mechanical cues that sperm encounter in vivo. As a result, these approaches fall short in evaluating functional sperm behavior related to rheotaxis, reducing their clinical and research utility[5,11].

In recent years, microfluidic technologies have emerged as versatile platforms for studying cellular biomechanical responses. This is largely due to their precise flow control and the ability to replicate physiological environments through biomimetic designs[12]. When adapted for sperm research, microfluidic systems enable real-time monitoring of rheotaxis under controlled shear forces and within confined geometries. These features closely mimic the in vivo conditions of the female reproductive tract[13,14]. However, most existing microfluidic devices rely on overly simplified channel architectures. They often ignore the presence of mucosal folds—anatomical structures known to influence sperm trajectories. In addition, the lack of standardized, quantitative metrics for assessing sperm rheotaxis remains a major obstacle. This limitation hinders the clinical translation of microfluidic platforms for fertility evaluation[15–18].

To address these limitations, we developed a bioinspired microfluidic platform that replicates the mucosal fold topology of the female reproductive tract. The device also incorporates tunable flow conditions, allowing real-time induction and observation of sperm rheotaxis under physiologically relevant shear environments. The system enlables quantitative evaluation of rheotactic behavior through a newly defined parameter: the Sperm Rheotaxis Index (SRI). The SRI offers a robust, sensitive, and physiologically relevant measure of sperm functional capacity, advancing both the mechanistic understanding of rheotaxis and its clinical application. By combining biomimetic design with quantitative assessment, this platform enhances the current toolkit for functional sperm diagnostics. It also introduces a new benchmark for early detection of male infertility and more nuanced evaluation of reproductive potential.

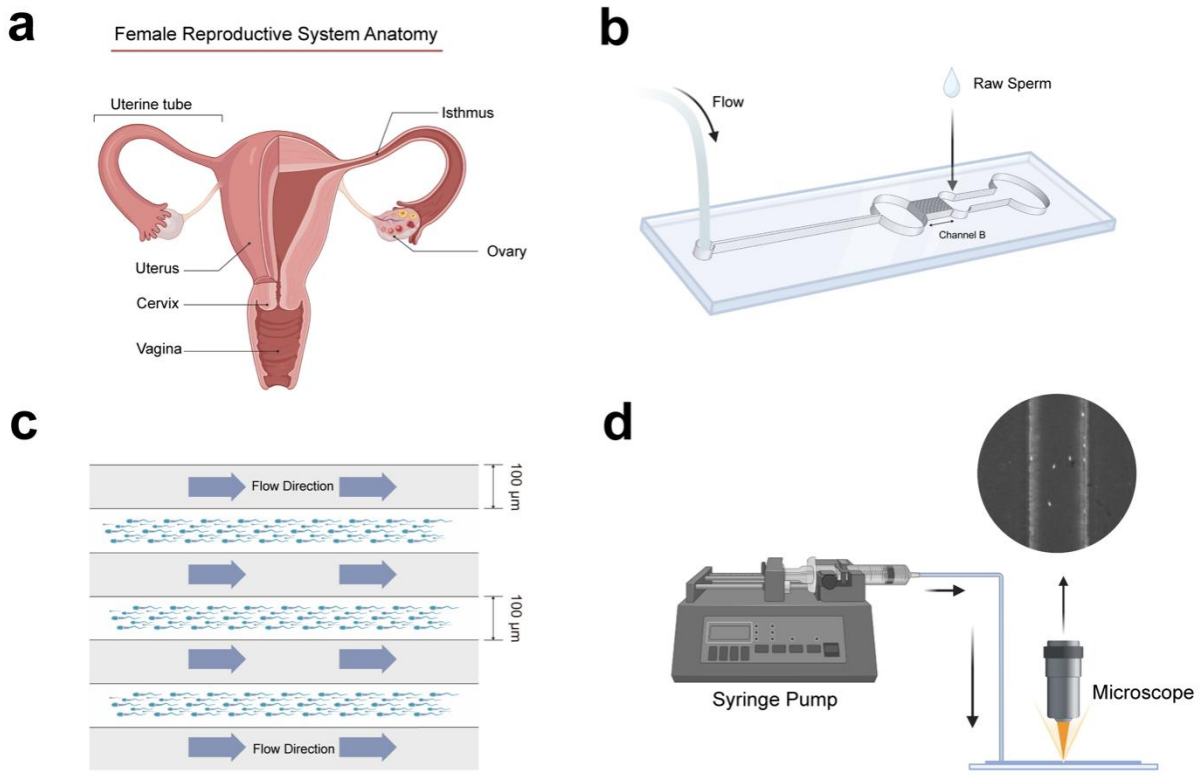


Figure 1. Female reproductive tract and microfluidic platform. a) Schematic of the female reproductive tract, where sperm undergo complex selection to reach and fertilize the oocyte. b) Microfluidic chip with chambers and interconnected channels; buffer is introduced via an inlet with extension tubing, and raw semen is added through the sample reservoir. c) In fence-like channel B, flow direction within the chip channels shows sperm swimming upstream against the flow via rheotaxis. d) Syringe pump controls a stable flow rate, and a microscopy system records real-time sperm motion in the channels.Picture was created by Biorender.

2.Results and discussion

2.1. Microfluidic Platform Inducing Sperm Rheotaxis

In the oviduct, mucosal folds run longitudinally and form crypts and grooves[19,20] , Some crypts are only tens of micrometers wide and can direct sperm movement[21]. Building on a previously reported channel architecture[22], We developed a microfluidic platform to replicate and quantify sperm rheotaxis in vitro. The modified microfludic chip mimics the folded inner wall of the female reproductive tract. The chip recreates this structure and produces a stable flow. Sperm with rheotactic ability can swim upstream against the flow. This setup captures key guidance cues seen in vivo.

The platform comprises a microscope, a syringe pump, a microfluidic chip, and connecting tubing. The chip consists of an inlet, three chambers, and interconnecting microchannels. And the overall height of the chip is 100 μm. The three chambers are with different functions. The collection chamber is 6 mm in diameter and gathers upstream-swimming sperm. The sample chamber is 4 mm in diameter and receives raw semen. The waste chamber is 8 mm in diameter and holds excess fluid. Microchannel B connects the sample and collection chambers. It is 5 mm long and contains parallel fence-like structures. These features mimic mucosal protrusions in the female tract and help guide sperm in a directional movement(Figure 1b).

To better mimic the female reproductive tract, we modified the design of Sandhya et al and reduced the spacing within the fence-like structure from 300 μm to 100 μm(Figure 1c) [22]. This optimized spacing more closely matches the reported dimensions of oviductal fold gaps, enhancing the biomimetic accuracy of the system[23]. And the modified design maintains the overall width of microchannel B. This change increases the number of available swimming lanes without altering the chip's global dimensions. Thusthe platform can better accommodate rheotactic sperm.

We used a syringe pump to provide a continuous, constant driving flow rate. (Figure 1d). Under these conditions, sperm entered the chip and moved upstream into the fence-like structures. Their movement was guided by both rheotaxis and the channel's surface features.This setup allows for precise in vitro simulation and quantification of sperm rheotaxis.

We used COMSOL Multiphysics to simulate flow velocity and shear rate at 0.5 μL/min (Figure 2a). For computational simplicity, water was used as the working fluid.The inlet-connected channels showed higher velocity and shear rate. This helped retain rheotactic sperm in the collection chamber (Figure 2b,d).We analyzed the fence-like microchannel in more detail. All swimming lanes had similar velocity and shear profiles (Figure 2c,e). Within each lane, velocity peaked at the center and dropped near the walls. Shear rate was lowest along the axis and at the corners (Figure 2c,e).

We used a phase-contrast microscope with a real-time image acquisition system to monitor sperm motility. The closely spaced swimming lanes allowed simultaneous observation of sperm across three adjacent lanes. Given the 100 μm channel height, sperm cells can swim across different z-planes, resulting in a depth-dependent variation in the number of cells that are visible and trackable within a single focal plane. To maximize the number of sperm that could be reliably resolved for sperm rheotaxis analysis, the focal plane

was adjusted along the z-axis prior to each acquisition to the plane with the highest sperm density and sufficient image contrast, and was maintained throughout each recording for a given field of view. Sperm were visible as bright head spots within the same field of view at constant magnification(Video S1).

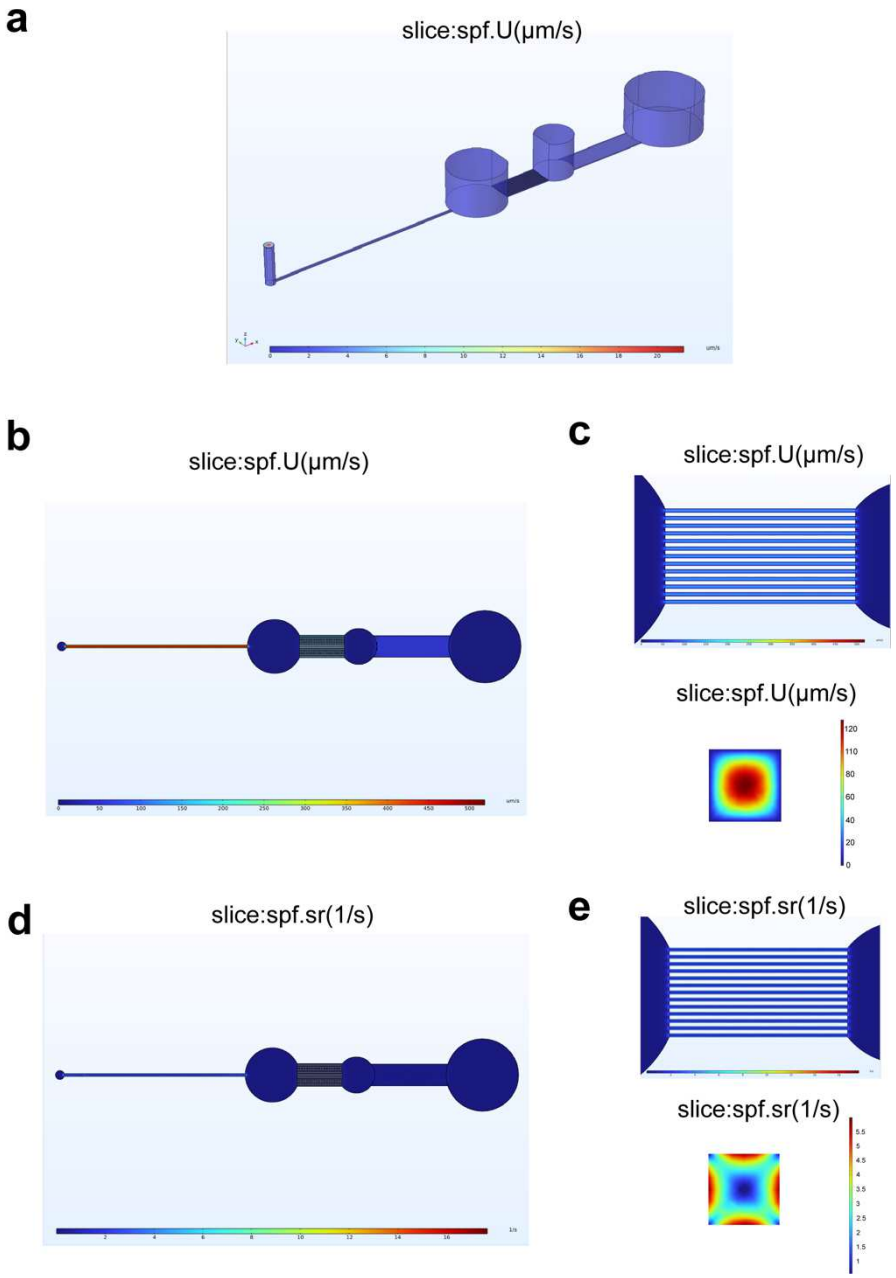


Figure 2. COMSOL simulation of fluid velocity and shear distribution. a) Three-dimensional velocity profile within the microfluidic chip channels. b) Fluid velocity across the entire chip. c) Fence-like channel B, including cross-sectional velocity distribution within a single lane. d) Sshear rate across the microchannel network. e) Fence-like channel B, highlighting cross-sectional shear rate patterns within an individual lane.

Based on COMSOL simulations and the known rheotactic behavior of sperm cells, we predict that sperm will tend to swim along the edges near the inner walls of each lane in microchannel B[24]. Due to consistent fluid dynamics across lanes and cross-sections, sperm distribution should be uniform throughout the channel. Therefore, rheotaxis can be reliably assessed by observing any randomly selected lane within the microscope's field of view.

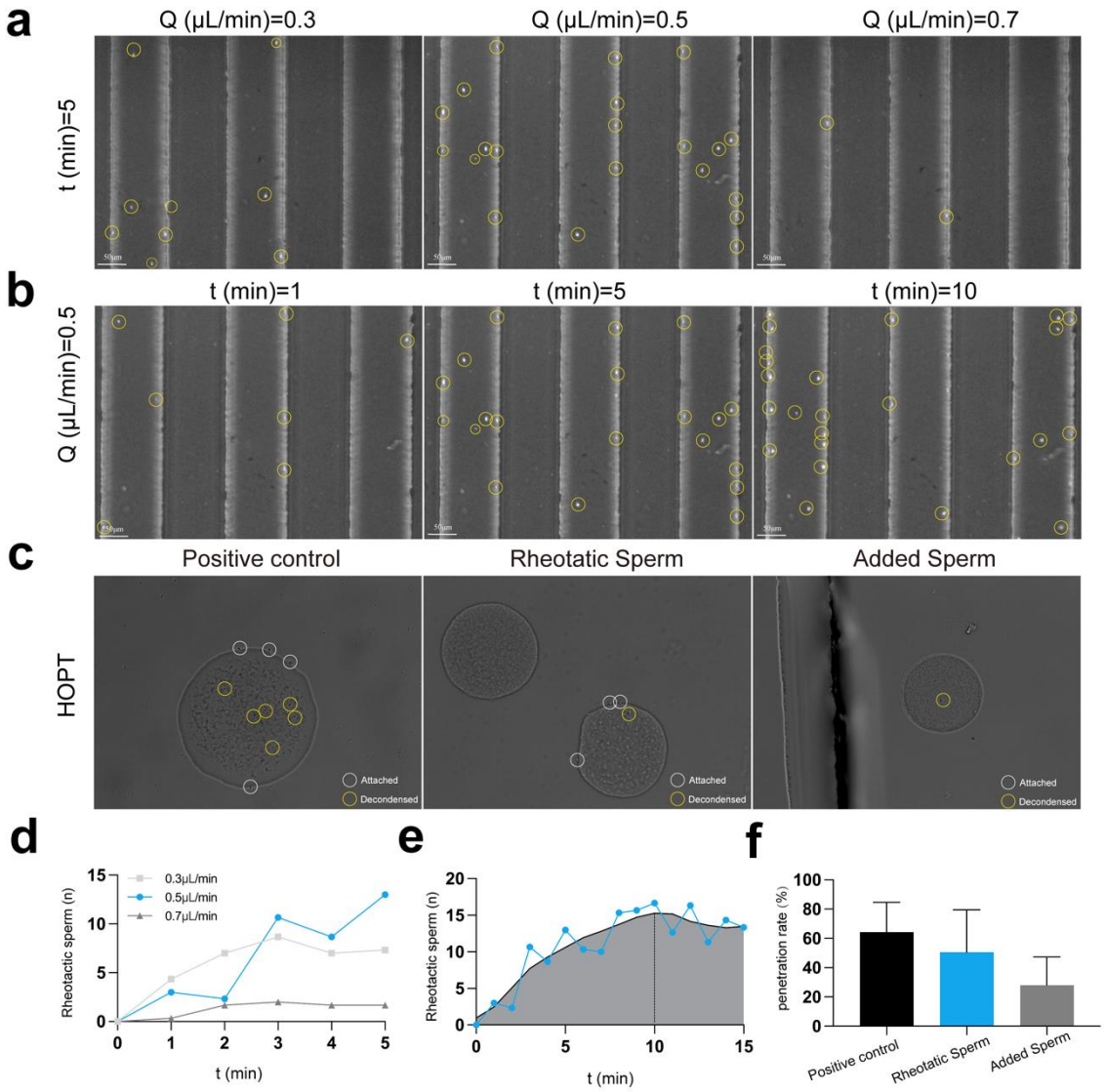


Figure 3. a) Sperm counts showing rheotactic movement in microchannels under varying flow rates (Q = 0.3, 0.5, and 0.7 μL/min). b) Time-dependent changes in rheotactic sperm counts at 0.5 μL/min flow rate. c) Oocyte penetration by sperm from the positive control, high-rheotaxis group, and chip-recovered samples. d) Temporal profiles of sperm counts under different flow conditions, showing the highest accumulation at 0.5 μL/min. e) Time course of sperm accumulation at 0.5 μL/min, peaking at 10 min. f) Comparison of oocyte penetration rates among positive control, rheotatic sperm, and added sperm groups.

178

179 *2.2. Microfluidic application and the Construction of Sperm Rheotaxis Index (SRI)*

180 Flow rate and observation timing were optimized to efficiently induce and monitor
181 sperm rheotaxis within the microfluidic platform. We tested three rates: 0.3, 0.5, and
182 0.7 μL/min (Figure 3a). At 0.7 μL/min, sperm had trouble entering the lanes and were pushed
183 away (Figure 3d). Sperm rheotaxis appeared within 5 minutes at 0.3 and 0.5 μL/min. The
184 0.5 μL/min condition led to more lane entry and stronger directional swimming. Based on
185 these results, we chose 0.5 μL/min as the optimal rate. Real-time imaging showed peak
186 rheotaxis 10 minutes after platform processing began (Figure 3b,e).

187 To quantify sperm rheotaxis, we defined the Sperm Rheotaxis Index (SRI) as the
188 maximum number of sperm exhibiting rheotaxis in the platform for each semen sample
189 (Figure S1). Evaluation was conducted at 0.5 μL/min, using images from three adjacent lanes
190 in channel B acquired between 10 and 11 minutes after processing began. Within this one-
191 minute interval, three frames were randomly selected for analysis. This random sampling
192 strategy was employed to reduce potential sampling bias arising from temporal fluctuations in
193 sperm distribution and motility, allowing us to obtain a more robust and representative
194 estimate of the rhrotatic sperm within the observation window.

195 To further assess the functional relevance of sperm rheotaxis, a zona-free hamster
196 oocyte penetration test (HOPT) was conducted. Sperm selected based on rheotaxis were
197 compared with non-rheotactic sperm (Figure 3c). The rheotactic group showed a higher
198 oolemma penetration rate ($N = 3$, $P > 0.05$) (Figure 3f). Although not statistically significant,
199 the trend supports a positive association between rheotaxis and fertilization potential.

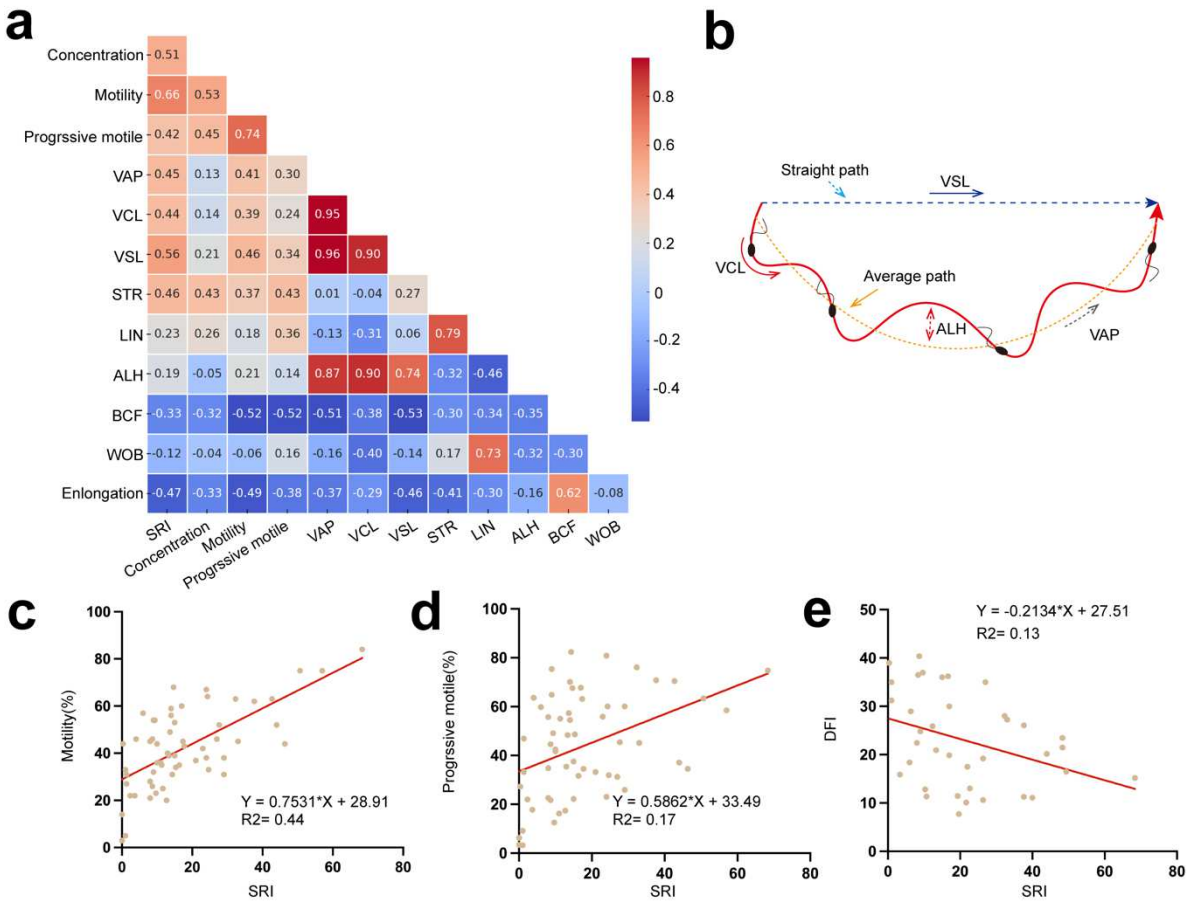


Fig. 4 a) SRI shows a significant positive correlation ($r > 0.4$) with sperm motility, STR, VSL, VCL, VAP, and progressive motility. b) CASA motility parameters of sperm. c) Positive correlation between SRI and sperm motility ($Y = 0.7531 \times X + 28.91$, $R^2 = 0.44$). d) Positive correlation between progressive motility and SRI ($Y = 0.5862 \times X + 33.49$, $R^2 = 0.17$). e) Negative correlation between SRI and sperm DFI, with regression equation $Y = -0.2134 \times X + 27.51$ ($R^2 = 0.13$).

2.3. Correlation of SRI with Sperm Concentration, Motility, and DNA Fragmentation Index (DFI)

Sperm concentration, motility, and DFI are key clinical parameters commonly used to assess semen quality, with well-established links to male fertility and ART outcomes [25]. We performed correlation analyses between SRI, sperm concentration, and various motility parameters. As shown in the heatmap, SRI exhibited moderate positive correlations ($r > 0.4$) with sperm concentration, motility, straightness (STR), straight-line velocity (VSL), curvilinear velocity (VCL), average path velocity (VAP), and progressive motility(Figure 4a-4d). In contrast, SRI showed a significant negative correlation with sperm head elongation rate ($r < -$

0.4) and only weak correlations with linearity (LIN), amplitude of lateral head displacement (ALH), and beat-cross frequency (BCF).

Interestingly, although SRI generally followed the same trend as sperm motility, correlation analysis revealed that some semen samples with relatively high motility exhibited low SRI values. Importantly, motility assessed by CASA parameters does not necessarily predict fertilization capacity or capture the role of the female reproductive tract in sperm selection[26]. As a form of directional motility, sperm rheotaxis likely reflects distinct physiological properties and underlying mechanisms compared to conventional motility. Therefore, SRI testing provides a valuable complement to conventional sperm functional assessments.

Also, SRI showed a significant negative correlation with DFI, suggesting that sperm DNA damage may impair rheotactic ability(Figure 4e). Reduced motility and elevated DFI are widely recognized as key indicators of diminished fertilization potential[27]. In this study, the consistent correlations of SRI with both motility parameters and DFI highlight its potential as a novel marker for sperm quality assessment. Moreover, as rheotaxis reflects a fundamental physiological trait, its quantitative evaluation via SRI may more accurately capture the fertilization capacity of sperm under physiological conditions.

2.4. SRI in the Diagnosis of Male Infertility

2.4.1. Baseline Characteristic

Between May 2024 and February 2025, 86 participants meeting the study criteria and providing informed consent were enrolled (CHEC021-086). Baseline data are summarized in Table 1. Median age was 31 years (range 19–49). All participants provided semen samples for routine analysis. Sperm concentration ranged from 4 to 294 million/mL (median 67.1 million/mL). Mean motility was 51.5% (SD 19.8%), and mean progressive motility was 45.1% (SD 20.0%). SRI values ranged from 0 to 68.3 (median 14).

Among the 86 enrolled patients, 22 (25.58%) were healthy individuals**.** A total of 47 patients (54.65%) were clinically diagnosed with male infertility, 28 patients (32.56%) with asthenozoospermia, 12 patients (13.95%) with varicocele, and 4 patients (4.65%) with oligozoospermia. All patients were recruited from the study institution.

Table 1. Baseline Characteristics of Patient Cohort

Variable	Value
Age, median (IQR), years	31 (27–34)
Abstinence period, median (IQR), days	3 (3–5)
Semen analysis	
Concentration, median (IQR), million/mL	67.1 (44.6–118.64)
Sperm motility (%), mean ± SD	51.54 ± 19.82
Progressive motility (%), mean ± SD	45.09 ± 19.96
Sperm Rheotaxis Index, median (IQR)	14 (8–24.33)
Clinical diagnosis, no (%)	
Health examination	22（25.58%）
Oligospermia	4（4.65%）
Asthenospermia	28（32.56%）
Male infertility	47（54.65%）
Varicocele	12（13.95%）

2.4.2. SRI and Semen Quality Among Different Patient Groups

Significant differences in age, sperm concentration, progressive motility, and SRI were observed across patient groups ($P < 0.05$; Table 2). Healthy controls showed notably higher SRI values compared to patients with infertility-related conditions, including oligozoospermia, asthenozoospermia, varicocele, and idiopathic infertility(Figure 5). These findings further support the notion that impaired sperm rheotaxis contributes to reduced fertility in these subgroups.

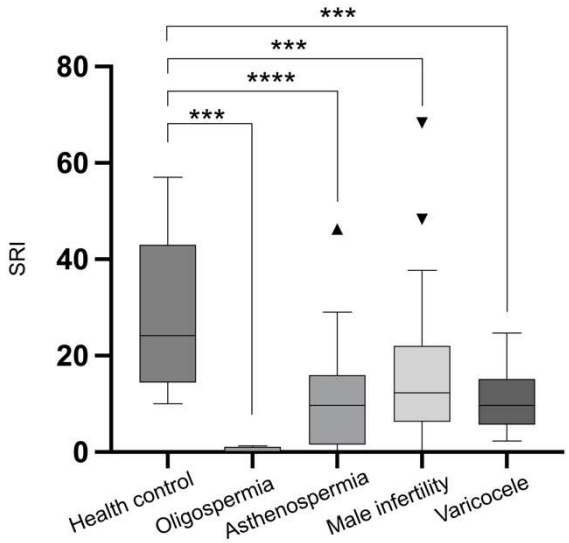


Figure 5. Comparison of SRI Across Different Disease Groups, Data are presented as Tukey boxplots.

259

Table 2. Comparison of Semen Quality and SRI Across Disease Groups

Variable	Health examination (n=22)	Oligospermia (n=4)	Asthenospermia (n=28)	Male infertility (n=47)	Varicocele(n=9)	H value	P value
Age, median (IQR), years	29 (26.25-34)	28.5 (27.75-32.5)	32.5 (28.5-34)	31 (29-34)	26 (23-26)	11.77	$P < 0.05$
Abstinence period, median (IQR), days	3 (3-4)	3.5 (2.28-4.5)	3.5 (3-5.25)	3 (3-4)	4 (3-5)	3.29	$P > 0.05$
Concentration, median (IQR), million/mL	111.32 (71.21-156.73)	9.24 (4.33-14.09)	55.32 (33.68-72.66)	65.47 (46.63-112.3)	64.16 (58.43-71.1)	23.83	$P < 0.05$
Sperm motility (%), mean ± SD	61.76 ± 12.54	38.33 ± 16.98	30.03 ± 10.89	50.72 ± 19.22	41.77 ± 20.67	39.41	$P < 0.05$
Progressive motility (%), mean ± SD	56.18 ± 12.56	20.96 ± 17.61	23.82 ± 9.97	45.39 ± 19.75	35.86 ± 18.06	42.59	$P < 0.05$
Sperm Rheotaxis Index, median (IQR)	24.17 (15.25-42)	0.17 (0-0.58)	9.67 (2.08-15.33)	12.33 (7.17-20.83)	9.67 (8.67-14)	27.94	$P < 0.05$

2.4.3. Receiver operating characteristic(ROC) analysis for infertility-related conditions

To further assess the clinical diagnostic value of the SRI, we evaluated its performance in identifying male infertility-related conditions (oligozoospermia, asthenozoospermia, varicocele, and idiopathic infertility). ROC curve analysis demonstrated that SRI outperformed sperm motility and progressive motility, achieving an area under the curve (AUC) of 0.77 (95% CI: 0.669–0.873) with an optimal cutoff of 9.83(Figure 6a). At this threshold, the sensitivity and specificity were 43.75% and 100%, respectively. Notably, among the subgroup with normal sperm motility, the diagnostic performance of motility parameters declined markedly, whereas SRI maintained robust discriminative capacity (AUC = 0.73, 95% CI: 0.597–0.855) (Figure 6b).

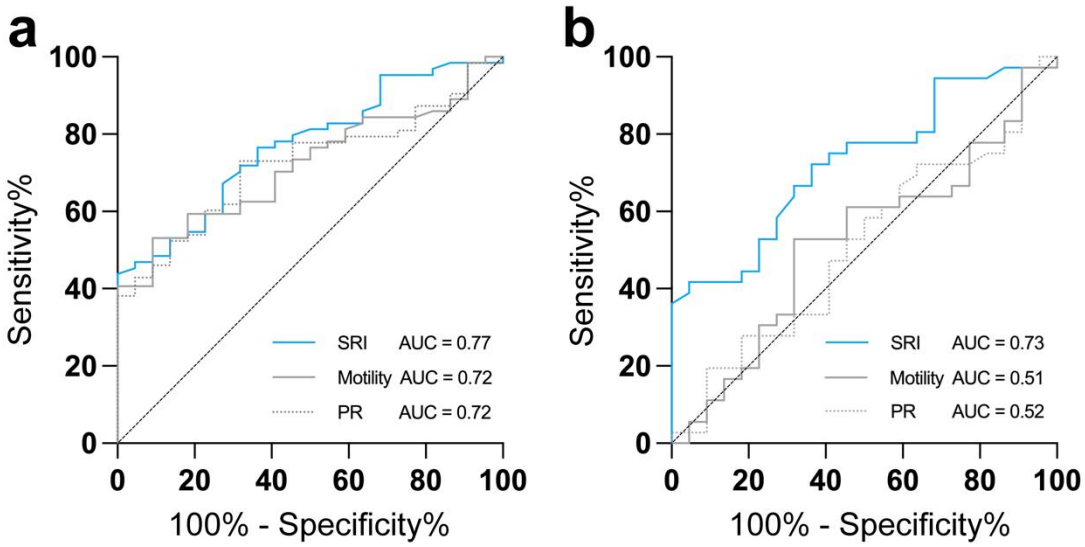


Figure 6. ROC Analysis of (SRI) and Motility Parameters. a) ROC analysis demonstrating the diagnostic performance of SRI (AUC = 0.77), outperforming both total motility(AUC = 0.71) and progressive motility (AUC = 0.71). b) Subgroup analysis in normo-motile sperm samples; SRI exhibits a significant diagnostic value (AUC = 0.73, $P < 0.05$), whereas total motility (AUC = 0.51) and progressive motility (AUC = 0.52) show limited diagnostic capacity ($P > 0.05$).

The newly-apdated WHO-defined reference values for sperm motility parameters reflect only the 5th percentile among fertile men, and exceeding them does not guarantee normal fertility[4,28]. While motility assessment helps distinguish fertile from infertile men, its diagnostic performance remains moderate, consistent with our findings[3]. By contrast, SRI showed superior

diagnostic value, effectively discriminating fertility status even among patients with normal motility, underscoring its clinical relevance.

Currently, a substantial proportion of infertile men lack a clearly defined cause, making comprehensive assessment of fertility potential critical for guiding more effective treatment strategies[4,29–31]. As an objective, quantitative measure of sperm rheotaxis, SRI provides an important complement to conventional sperm function tests. Clinically, SRI shows strong potential as a diagnostic tool for identifying high reproductive risk conditions and evaluating male fertility potential, offering a novel biomarker for assisted reproduction and infertility management. By assessing sperm rheotaxis, this approach challenges the traditional paradigm focused solely on motility, delivering new insights into male infertility mechanisms and advancing precision medicine.

The main limitations of this study are the relatively small sample size and the absence of multicenter cross-validation. Additionally, the study did not compare the diagnostic performance of sperm morphology assessment or DFI with that of SRI. In clinical practice, sperm DFI testing and morphological evaluation are limited by higher costs and labor intensity, and they are typically conducted only in high-risk fertility populations or patients already diagnosed with male infertility, introducing potential selection bias. Therefore, these parameters were not included in the comparative diagnostic analysis.

3. Conclusion

We developed a microfluidic platform capable of inducing stable sperm rheotaxis under well-defined flow conditions, enabling the selective isolation and quantitative assessment of highly rheotactic sperm. The channel dimensions, geometry, and flow profiles were designed to mimic key anatomical features of the mucosal folds in the female reproductive tract. Through real-time imaging and streamlined analysis, we established the SRI as a quantitative metric for characterizing sperm rheotactic behavior. The SRI assay can be completed within approximately 15 minutes, offering a rapid and efficient approach for functional sperm assessment. Importantly, SRI quantification relies only on standard bright-field imaging and can be implemented using existing CASA systems, facilitating integration into current laboratory workflows. While the present prototype represents a laboratory-based implementation, ongoing engineering efforts toward simplified and user-friendly operation are expected to further support its clinical translation. Overall, SRI shows strong potential as a screening tool for evaluating sperm physiological function and infertility-related conditions, and as a novel indicator for male fertility assessment.

4. Materials and methods

4.1 Device fabrication

The chip mold was fabricated using photolithography, where the design was transferred onto a silicon wafer coated with SU-8 photoresist. A uniform SU-8 layer（Shengquan, Jinan, China） was spin-coated at 500 rpm for 9 seconds and 1800 rpm for 20 seconds. After coating, the wafer was soft-baked on a hot plate at 65°C for 15 minutes and 95°C for 20 minutes, exposed to UV light through a channel mask for 30 seconds, and post-baked to solidify the pattern.Polydimethylsiloxane (PDMS, Momentive, USA) was used for chip construction. PDMS base and curing agent were mixed at a 10:1 weight ratio, thoroughly stirred, degassed under vacuum, and centrifuged at 1200 rpm for 5 minutes. The mixture was poured onto the mold to ~4 mm thickness, left to stand for 10 minutes, and cured at 80°C for 30 minutes. After curing, the PDMS slab was demolded, trimmed, and punched with inlet/outlet holes. Both the PDMS block and a glass slide were cleaned, plasma-treated, bonded, and heated at 85°C for 30 minutes to strengthen adhesion.

4.2 Medium

A modified human tubal fluid solution was used to maintain optimal physiological pH for sperm within the microfluidic chip. The medium contained NaCl (94.66 mM), KCl (4.78 mM), KH_2PO_4 (1.19 mM), $NaHCO_3$ (4.15 mM), $MgSO_4 \cdot 7H_2O$ (1.19 mM), $CaCl_2 \cdot 2H_2O$ (1.71 mM), HEPES buffer (20.85 mM), glucose (5.56 mM), sodium pyruvate (0.33 mM), sodium lactate (23.28 mM), gentamicin (0.025 g/L), phenol red (0.010 g/L), and bovine serum albumin (4.0 g/L) dissolved in 1000 mL deionized water (pH 7.4).

4.3 Study population

From May 2024 to February 2025, semen samples were collected from 86 patients at Shanghai Changhai Hospital. Clinical data, including birth date, fertility history, semen analysis results, medical history, and spouse’s medical history, were recorded. The study was approved by the institutional ethics committee (CHEC021-086), and informed consent was obtained from all participants. The study was conducted in accordance with the principles outlined in the Declaration of Helsinki. Inclusion criteria: (1) males aged 18–50 years; (2) 2–7 days of abstinence before sample collection; (3) ability to provide semen by masturbation following standardized protocols; (4) signed informed consent. Exclusion criteria: (1) age <18 years; (2) ejaculatory dysfunction or inability to provide semen; (3) non-liquefied or delayed liquefied samples; (4) azoospermia; (5) severe systemic illness (e.g., advanced cancer, severe cardiovascular/cerebrovascular disease, coagulation disorders); (6) sexually transmitted infections (e.g., syphilis, HIV); (7) any condition deemed unsuitable by the investigators.

4.4.Semen Sample Processing

Samples were collected by masturbation and incubated at 37°C for 30 minutes for liquefaction before analysis and processing.

4.5. Experimental Setup

The microfluidic platform was integrated with an image capture system. Before use, the sample and collection chambers were sealed with transparent tape. A 5 mL syringe filled with 2 mL of pre-warmed (37°C) modified HTF solution was connected to the chip inlet via a disposable extension tube. The syringe, mounted on a pump (LSP02-2A, Longer, Baoding, China), was used to fill all channels except the waste chamber, displacing air. The flow rate was set to 0.6 mL/h. After removing the sample inlet tape, 15 μL of liquefied semen was added, and the chamber was resealed. The chip was placed on a CASA system (HT-IVOS II, Hamilton Thorne, USA) with a 37°C heated stage. A 10× objective was used, and the field was adjusted to display at least three lanes. Along the z-axis, the focal plane was adjusted before each acquisition to the plane with the highest sperm density and sufficient image contrast, and was kept fixed throughout the recording. Sperm movement was recorded for analysis at 5 fps, minimum resolution 640 × 480 pixels. To collect the sorted sperm from the chip, the tape on both the sample and collection chambers was removed. Channel B was sealed at both ends using flat tweezers, and the sperm sample was extracted with a pipette.

4.6. COMSOL analysis

Fluid flow within the microchannels was simulated using COMSOL Multiphysics. The flow in the microfluidic structure was set as steady, incompressible, and Newtonian, using water as the working fluid. A constant volumetric flow rate (Q = 0.5 μL/min) was applied at the channel inlet, while a zero-pressure condition was applied at the outlet. No-slip boundary conditions were imposed on all channel walls.Under these boundary constraints, the Navier–Stokes equations were solved to obtain the velocity field and shear rate distribution within the channels.

4.7. HOPT Analysis

Zona-free hamster oocytes (Antimo, Nanjing, China) were used after thawing and removal of the zona pellucida with trypsin (Sigma-Aldrich, USA). Semen samples with normal motility were divided into groups: positive control (processed by sperm gradient separation) and experimental groups (sperm collected from the collection and sample chambers after 30-minute microfluidic selection). Sperm were centrifuged, diluted to 1×10^6/mL, and capacitated by incubation with calcium ionophore (A23187, Eason, Shanghai, China) for 3 hours. At least five oocytes were co-incubated at 37°C in 5% CO_2 for 3 hours.

After washing, oocytes were examined under a phase-contrast microscope, and the number of decondensed sperm heads and penetration rates were recorded.

4.8. Velocity Analysis

Sperm concentration and motility were analyzed using a CASA system (HT-IVOS II, Hamilton Thorne, USA). Semen samples were placed in a 37°C water bath for 30 minutes to ensure complete liquefaction. A 4 μL aliquot was loaded onto a disposable analysis chamber. At least 200 sperm per sample were evaluated.

4.9 DNA Fragmentation

DNA fragmentation was measured using an acridine orange staining kit (Prism-Tek, Chengdu, China). After liquefaction, a 10 μL semen aliquot was diluted in 90 μL Tris buffer, mixed, treated with 200 μL of 0.1% Triton X-100 for 30 seconds, and stained with 500 μL acridine orange for 3 minutes. Flow cytometry was used to analyze at least 5,000 sperm per sample, identifying the P1 and P2 populations and quantifying high DNA stainability (HDS) and DFI.

4.10 SRI Analysis

Sperm rheotaxis was evaluated using the microfluidic platform. A syringe with buffer was connected and used to fill all channels (except the waste chamber), displacing air. The flow rate was set at 0.6 mL/h. After adding 15 μL liquefied semen and resealing, the chip was placed on the CASA stage with a 10× objective. The field was adjusted to show at least three lanes, and the flow rate was set to 0.5 μL/min. Sperm movement was recorded between 10 and 11 minutes after adjustment. Using Fiji software, sperm within the microchannels were counted and used to calculate the sperm rheotaxis index (SRI).

4.11 Statistical Analysis

Analyses were conducted using SPSS v27.0 (SPSS Inc., USA). Normally distributed data were expressed as mean ± SD and range; non-normal data were shown as median (interquartile range). Categorical variables were reported as counts and percentages. Group differences were assessed using the Mann–Whitney U test, Wilcoxon signed-rank test, or Kruskal–Wallis test. Diagnostic performance was evaluated using ROC curves, with AUC calculated. Optimal cutoff values were determined by the Youden index. A p-value < 0.05 was considered statistically significant.

Conflict of interest

The authors declare that they have no known competing financial interests or personal relationships that could have appeared to influence the work reported in this paper.

Acknowledgements

This work was supported by the Establishment of a Male Fertility Protection System, the Establishment and Application of Testicular Biochips, Protection and evaluation of complex electromagnetic radiation.

Data availability

Data will be made available on reasonable request.

References

1. Vander Borght, M. & Wyns, C. Fertility and infertility: Definition and epidemiology. *Clin Biochem* **62**, 2–10 (2018).
2. Cannarella, R. & Calogero, A. E. Male infertility: from etiology to management. *Minerva Endocrinol (Torino)* **47**, 1–3 (2022).
3. Guzick, D. S. *et al.* Sperm morphology, motility, and concentration in fertile and infertile men. *N Engl J Med* **345**, 1388–1393 (2001).
4. Fraga, L. G. *et al.* Clinical and Laboratorial Evaluation of Male Infertility. A Detailed Practical Approach. *Arch Med Res* **55**, 103139 (2024).
5. Khatun, A., Rahman, M. S. & Pang, M.-G. Clinical assessment of the male fertility. *Obstet Gynecol Sci* **61**, 179–191 (2018).
6. Sakkas, D., Ramalingam, M., Garrido, N. & Barratt, C. L. R. Sperm selection in natural conception: what can we learn from Mother Nature to improve assisted reproduction outcomes? *HUMAN REPRODUCTION UPDATE* **21**, 711–726 (2015).
7. Williams, M. *et al.* Recovery of artificially inseminated spermatozoa from the fallopian tubes of a woman undergoing total abdominal hysterectomy. *Hum Reprod* **7**, 506–509 (1992).
8. Cerezales, S., Boryshpolets, S. & Eisenbach, M. Behavioral mechanisms of mammalian sperm guidance. *Asian J Androl* **17**, 628 (2015).
9. Miki, K. & Clapham, D. E. Rheotaxis Guides Mammalian Sperm. *Current Biology* **23**, 443–452 (2013).

10. Romero-Aguirregomezcorta, J. *et al.* Sperm selection by rheotaxis improves sperm quality and early embryo development. *Reproduction* **161**, 343–352 (2021).
11. Sigman, M., Baazeem, A. & Zini, A. Semen analysis and sperm function assays: what do they mean? *Semin Reprod Med* **27**, 115–123 (2009).
12. Hajam, M. I. & Khan, M. M. Microfluidics: a concise review of the history, principles, design, applications, and future outlook. *Biomater. Sci.* **12**, 218–251 (2024).
13. Ahmadkhani, N., Hosseini, M., Saadatmand, M. & Abbaspourrad, A. The influence of the female reproductive tract and sperm features on the design of microfluidic sperm-sorting devices. *J Assist Reprod Genet* **39**, 19–36 (2022).
14. Nosrati, R. *et al.* Microfluidics for sperm analysis and selection. *Nat Rev Urol* **14**, 707–730 (2017).
15. Abdel-Ghani, M. A., El-Sherry, T., Mahmoud, G. & Nagano, M. Implications of ram sperm rheotaxis analysed by microfluidics for fertility. *Reprod Domest Anim* **55**, 1541–1547 (2020).
16. Tasoglu, S. *et al.* Exhaustion of racing sperm in nature-mimicking microfluidic channels during sorting. *Small* **9**, 3374–3384 (2013).
17. El-Sherry, T. M., Abdel-Ghani, M. A., Abdel Hafez, H. K. & Abdelgawad, M. Rheotaxis of sperm in fertile and infertile men. *Syst Biol Reprod Med* **69**, 57–63 (2023).
18. Zhang, Z. *et al.* Human sperm rheotaxis: a passive physical process. *Sci Rep* **6**, 23553 (2016).
19. Suarez, S. S. Mammalian sperm interactions with the female reproductive tract. *CELL AND TISSUE RESEARCH* **363**, 185–194 (2016).
20. Koyama, H. *et al.* Mechanical Regulation of Three-Dimensional Epithelial Fold Pattern Formation in the Mouse Oviduct. *Biophys J* **111**, 650–665 (2016).

21. Mullins, K. J. & Saacke, R. G. Study of the functional anatomy of bovine cervical mucosa with special reference to mucus secretion and sperm transport. *Anat Rec* **225**, 106–117 (1989).
22. Sharma, S., Kabir, Md. A. & Asghar, W. Selection of healthy sperm based on positive rheotaxis using a microfluidic device. *Analyst* **147**, 1589–1597 (2022).
23. Yániz, J. L., Lopez-Gatius, F., Santolaria, P. & Mullins, K. J. Study of the functional anatomy of bovine oviductal mucosa. *Anat Rec* **260**, 268–278 (2000).
24. Giojalas, L. C. & Guidobaldi, H. A. Getting to and away from the egg, an interplay between several sperm transport mechanisms and a complex oviduct physiology. *Mol Cell Endocrinol* **518**, 110954 (2020).
25. Liu, K., Mao, X., Pan, F., Chen, Y. & An, R. Correlation analysis of sperm DNA fragmentation index with semen parameters and the effect of sperm DFI on outcomes of ART. *Sci Rep* **13**, 2717 (2023).
26. Wang, C. & Swerdloff, R. S. Limitations of semen analysis as a test of male fertility and anticipated needs from newer tests. *Fertil Steril* **102**, 1502–1507 (2014).
27. Li, M.-W. & Lloyd, K. C. K. DNA fragmentation index (DFI) as a measure of sperm quality and fertility in mice. *Sci Rep* **10**, 3833 (2020).
28. Chawre, S. *et al.* A Review of Semen Analysis: Updates From the WHO Sixth Edition Manual and Advances in Male Fertility Assessment. *Cureus* https://doi.org/10.7759/cureus.63485 (2024) doi:10.7759/cureus.63485.
29. Pozzi, E. *et al.* Contemporary Diagnostic Work-Up for Male Infertility: Emphasizing Comprehensive Baseline Assessment. *World J Mens Health* https://doi.org/10.5534/wjmh.240069 (2024) doi:10.5534/wjmh.240069.
30. Kızılay, F. & Altay, B. Sperm function tests in clinical practice. *Turk J Urol* **43**, 393–400 (2017).

31. Oehninger, S., Franken, D. R., Sayed, E., Barroso, G. & Kolm, P. Sperm function assays and their predictive value for fertilization outcome in IVF therapy: a meta-analysis. *Hum Reprod Update* **6**, 160–168 (2000).